INTERNATIONAL JOURNAL OF PRECISION ENGINEERING AND MANUFACTURING Vol. 15, No. 2, pp. 267-273 FEBRUARY 2014 / 267
DOI: 10.1007/s12541-014-0334-9

Wire Tension Method for Coefficient of Friction Measurement of Micro Bearing

Hyung Jin Kim[1], In Kyum Park[1], Young Ho Seo[1], Byeong Hee Kim[1,#], and Nam Pyo Hong[2]

1 Dept. of Mechanical and Mechatronics Engineering, Kangwon National University, Chuncheon, Gangwon-do, South Korea, 200-701
2 Kangwon human Resources Development Institute, 165-1 Junghwagye-ri, Bukbang-myeon, Hongcheon-gun, Gangwon-do, South Korea, 250-885
Corresponding Author / E-mail: kbh@kangwon.ac.kr, TEL: +82-33-250-6374, FAX: +82-33-259-5551

KEYWORDS: Bearing tester, Wire tension method, Coefficient of friction, Micro bearing

In this paper, the novel bearing tester was developed by new method using a wire tension to obtain the coefficient of friction (COF) of micro bearings. Because the conventional bearing testers mostly use bulky and friction-nature torque sensors, there is a limitation to measure the minute rotational torques of the micro bearings. In order to overcome the previous limitation and estimate the COFs of very small journal bearings (inner diameter < 10 mm), the bearing was placed freely along the x-axis and the tension of the wire which wrapped the bearing and was connected between the counterweight and the load cell was measured. The COFs were calculated by dividing the radial friction force obtained by the wire tension by the initial vertical load given by the mass of the counterweight and the bearing module. The developed bearing tester could measure the COFs of the micro journal bearing of various shape and size effectively. The validity of the bearing tester was verified by several friction measuring tests. The system also showed very high repeatability and precision.

Manuscript received: November 12, 2013 / Accepted: December 31, 2013

NOMENCLATURE

u = COF (coefficient of friction)
F_N = normal force on the bearing
F_f = friction force between the shaft and the bearing
F_L = force on the load cell
R_b = radius of the shaft
R_L = radius of the bearing housing
ΣM_O = sum of the moments applied to the system
mg = directional orientation of the system

1. Introduction

Recently, research has been actively conducted on various types of fuel economy improvements in the car industry. In keeping with this trend, bearings have found wide application not only in cars but also in many other areas, including home appliances. In particular, the trends of miniaturization, precision, and high speeds in rotating equipment have driven the manufacture of bearings toward smaller and more accurate dimensions.[1-4] Recently developed power generation facilities have increased their power generation capacity owing to the increase in facility usage and the maximization of power trade revenue. In addition, daily or weekly starting and stopping operations have become more frequent than in the past as a result of the power demand variance. Owing to these circumstances, the operation conditions of bearings, which are critical elements in many devices used in industrial sectors, have become even more strenuous. Since high-speed rotating equipment is supported by bearings, the operational characteristics of bearings play a critical role in the operational reliability of equipment.[5,6] Abrasion, corrosion, electrical erosion, fatigue, overheat, and friction are the main types of damage that can occur. Among these types of damage, the friction of bearings has received considerable attention in precision engineering sectors.[7-10] When these types of damage are observed, the damage shapes are visually inspected and the symptoms are disclosed in laboratories. However, it is difficult both to estimate bearing life expectancy and observe and analyze the bearing's characteristics. Hence, many studies recently have been conducted on the friction of bearings.

In the test rig used by Yao et al., the journal of micro bearing is connected to the principle axis of the motor whose rotation can be easily modulated. Normal contact of a split bearing with a journal is

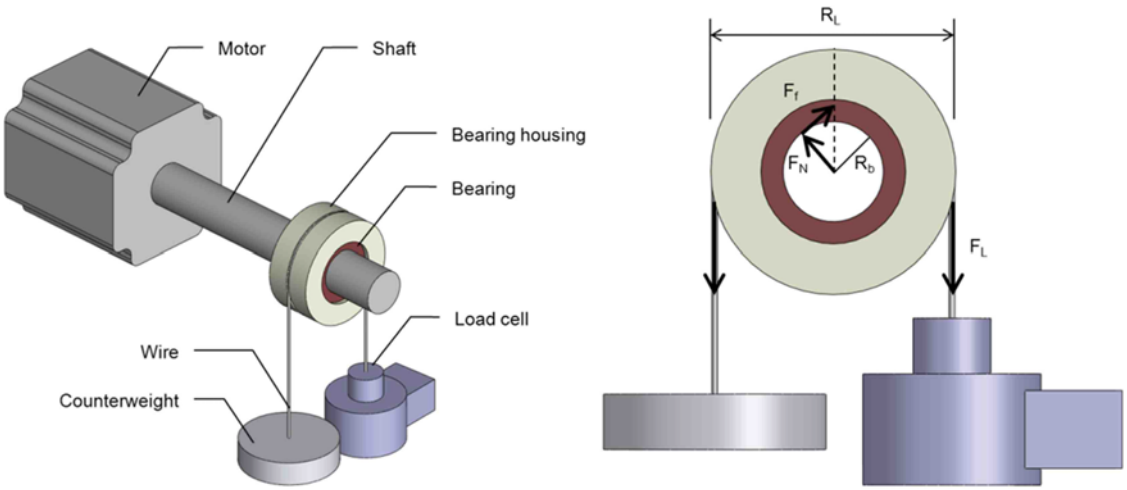

Fig. 1 Schematic representation of the force details of bearings and the wire

achieved using the cable brake principle, while the friction of the micro bearing is measured from the force difference at the two endsof the cable due to friction torque during running.[8] Tevruz's test rig was governed by the belt-hoop mechanism and consisted of a steel shaft supported by a rolling bearing, another tip that had a journal bearing sample, and a moment bar. The moment caused by the rotary journal maintained its balance by balancing weight. Further, normal force in the system was applied using a suspended load. The friction coefficient was calculated based on the diameter, and the normal force was calculated from the ratio of the friction moment.[11] Ünlü and Atik published a paper on the measurement of the friction coefficient of journal bearings. They developed a new test rig and method to measure the friction coefcient of a journal bearing, but they were not interested in the friction at start-up.[12] Bouyer conducted a study on journal bearings, including their static friction coefficient, and their equipment measured the bearing's friction force using a torque meter.[13] Rezaei developed a device to measure the friction of a bearing with an inner diameter of 300 mm using a load cell. This device measured the friction force between a bearing and a shaft, the bearing's temperature, and the wear rate of the bearing surface. The friction torque was measured by a load cell, as a force acted upon a lever arm connected to a bush.[14] Lee et.al. used the tribotester of disk on disk type. The tribotester was mainly comprised of an air cylinder, two load cells and a servo motor. The magnitude of the normal force was measured by a load cell installed under the air cylinder. The friction force was induced by the combination of the rotating motion and the normal load and was measured by another load cell located in the closed chamber.[15]

Tests on standard specimens of materials or technologies, aimed at measuring the friction coefficient and wear rate of products such as bearings, are performed by using standard tests, such as pin-on-disk (as outlined by ASTM G99) and specialized tester using real products.[16-18] Most bearing performance tests are conducted by using a torque sensor, which has a large volume.[19,20] In this study, a bearing friction test that does not use a torque sensor was devised for friction tests on various types of bearings used in the industrial sectors. The tester introduces a new method that can be used to reduce the overall system volume. It allows portability and can test bearings with various diameters. To achieve this, a tester was developed to measure the bearing's friction when radial load was applied, by using a wire tension method.

2. Measuring principle and bearing tester

2.1 Operation principle

The principle of the wire tension method used to measure the bearing friction is shown in Fig. 1. The wire is wound once around the bearing housing and fixed in place, a counterweight is connected at one end of the wound wire to apply radial load to the bearing, and a load cell is connected at the other end. The friction force of the bearing is generated when the shaft is rotated in the counterclockwise direction by the motor and the weight applies the initial tension to the wire. The contact point between the shaft and the bearing is aligned with the direction of the normal force on the bearing, F_N. The COFs of the bearing is expressed by Eq. (1):

$$\mu = \frac{F_f}{F_N} \tag{1}$$

where u is the bearing COFs generated during shaft rotation, F_N is the normal force on the bearing, and F_f is the friction force between the shaft and the bearing. F_N and F_f can be represented by the moment with respect to the shaft center, applied between the shaft and the bearing. Eq. (2) gives the sum of the moments applied to the system:

$$\Sigma M_o = -F_f R_b + mgR_b - F_L R_L = 0 \tag{2}$$

where F_L is sum of the wire tension generated during the shaft revolution and the initial tension due to the counterweight as the force on the load cell, R_b is the radius of the shaft, and R_L is the radius of the bearing housing.

Rewriting Eq. (2) in terms of F_f, the friction force between the shaft and the bearing can be represented by Eq. (3):

$$F_f = \frac{R_L}{R_b}(F_L - mg) \tag{3}$$

F_N is applied at the intersection between the shaft and the bearing while the shaft is rotated, and is perpendicular to F_f, i.e., the friction

force between the shaft and the bearing. Hence, it can be represented by the counterweight (mg) and the load cell load (F_L) as shown in Eq. (4):

$$F_N^2 = \left[\frac{R_L}{R_b}(F_L - mg)\right]^2 = (mg + F_L)^2 \quad (4)$$

$$F_N^2 + F_f^2 = (mg + F_L)^2 \quad (5)$$

$$F_N = [(mg + F_L)^2 - F_f^2]^{1/2} \quad (6)$$

$$\mu = \frac{\frac{R_L}{R_b}(F_L - mg)}{\left[(mg + F_L)^2 - \frac{R_L}{R_b}(F_L - mg)^2\right]^{1/2}} \quad (7)$$

The COFs between the shaft and the bearing can be represented by Eq. (7), obtained by substituting for F_f and F_N with Eq. (3) and (6), respectively, in Eq. (1).[13]

The principle underlying the measurement of the COFs of the micro-bearing can be explained as follows: the load generated by the wire (wound around the micro-bearing) connected to the counterweight and the friction force generated by the motor rotation are measured as the tension of the wire fixed to the load cell, thereby converting them to the COFs. Thus, the static and kinetic COFs between the shaft and the bearing bore inside the main bearing part can be measured.

2.2 Design and manufacture

In the present study, the COFs of a micro-bearing was measured using the wire tension method to evaluate its performance. Fig. 2 shows the schematic view of the bearing tester that uses the proposed wire tension method. The dimensions of the bearing tester were 420 (width) × 315 (length) × 400 (height) mm. It was designed as a miniaturized system to be operated in narrow spaces and in various operation environments, such as a constant-temperature and constant-humidity chamber or a low-temperature chamber. The structure was manufactured by machining the aluminum profile (20×20) and an aluminum plate (Al 6063).

The bearing tester was divided into three parts: a motor part, a sensor part, and a control part. The diameter of the rotation axis in the servomotor (Sanyo denki Co. Ltd., R2AA06020FXH00) used in the bearing tester was 14 mm. The tester was connected to the shaft using coupling (Misumi Inc. SCXW34-12-14). The motor could run at speeds between 10 and 6,000 RPM, and could operate in continuous or repetitive modes to enable various operation tests.

The sensor part was designed to make assembly and disassembly easier for test bearings of various sizes by separating independently, using the linear motion guide to move along the x-axis. The sensor part used three bearings of the same type for bearing testing: one main bearing that measured the bearing COFs, and two guide bearings that measured the temperature and supported the bearing shaft. Fig. 3 shows the design and photograph of the sensor part. The two guide bearings for axis support were designed to support various sizes of bearings with an outer diameter of 6~30 mm using a V shaped clamp. One side of the V-shaped clamp of the screw type was manufactured with a right-hand thread and the other side was manufactured with a left-hand thread, so that various sizes of bearings could be supported by rotating the clamp

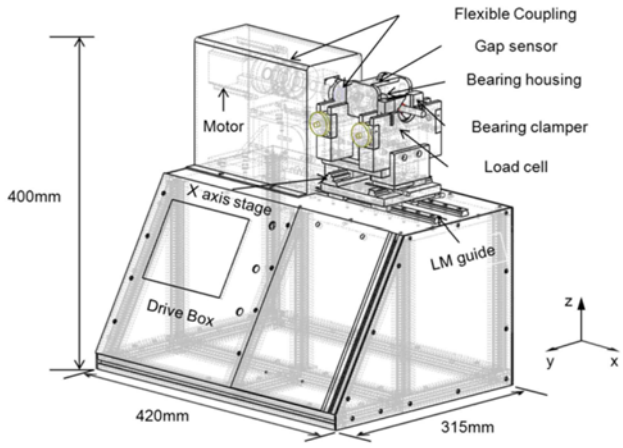

Fig. 2 Dimension of designed schematic view of the bearing tester

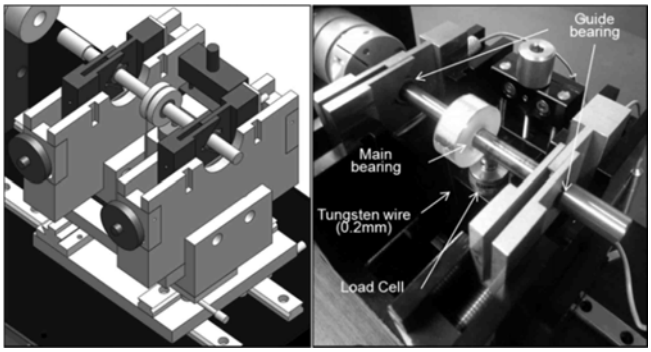

Fig. 3 design and photograph of the sensor part in the tester

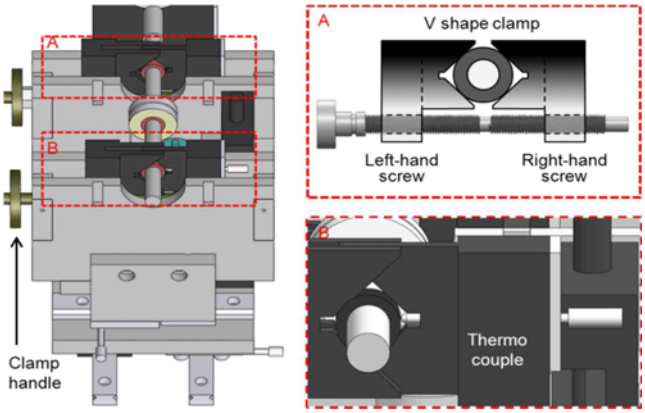

Fig. 4 Design of the screw-type V-shaped clamp attachment and the temperature sensor

handle in one direction. In addition, a hole was processed in the V-shaped clamp in order to measure temperature for the durability test. This allowed the temperature sensor physical contact with the two secondary bearings in order to measure the bearing temperature generated during shaft rotation. Fig. 4 shows the design of the screw-type V-shaped clamp attachment and the temperature sensor. A tension load cell was used to measure the COFs of the bearing. The COFs between the shaft and the bearing was calculated using the wire tension generated during the bearing shaft rotation and the initial tension due to the counterweight.

Table 1 Specifications of the parts used in the bearing tester

Part	Model	Specification	Unit
Motor	Sanmotion R R2AA06020FXH00	6000 (max.)	RPM
Load cell	WMC miniature sealed stainless steel load cell	4.54	kgf
Thermo couple	ITS-90	-260~1250	°C
Gap sensor	SD-8MS-SD	Resolution 0.001	mm
Wire	Tungsten	0.2	ϕ

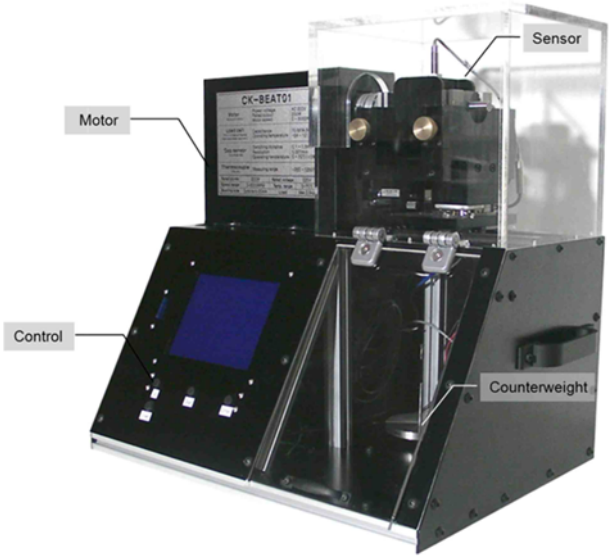

Fig. 5 External appearance of the manufactured bearing tester

The control part consisted of a liquid crystal display (LCD) window that could observe the status of the bearing tester, and four keys - Up, Down, Digit, and Enter - to control the operation mode of the motor, rotation speed, and time. It could also be used to input the weight (mg), bearing shaft radius (R_b), and bearing housing radius (R_L), in order to convert the bearing COFs. Although the input of information for the bearings to be tested and the starting and stopping Table 1 Specifications of the parts used in the bearing tester of the motor could be performed using the four buttons in the control part, a Labview-based operation program was also developed in order to perform the operation and monitoring of the bearing tester when it was placed in a narrow space such as a chamber. The bearing tester was designed and manufactured so as to enable data transfer through the system and storage in a personal computer (PC), as well as to enable data storage in an SD card.

Table 1 summarizes the specifications of the parts used in the bearing tester, and Fig. 5 shows the external appearance of the manufactured bearing tester. In order to minimize the motor noise, the interior of the aluminum case was treated with a soundproofing agent. To prevent bearing damage owing to the motor rotating at high speed, acryl of 8 mm thickness was used to protect the sensor part. Additionally, an emergency button was installed on the left side of the bearing tester in order to stop the motor in case of an emergency-bearing damage during high-speed rotation.

3. Experiment and Results

The bearing used in the experiment was an oil-impregnated sintered bearing whose chemical composition is shown in Table 2. The inner and outer diameters and width of the bearing were Table 2 The chemical composition of bearing (wt%) approximately 8, 12, and 5 mm, respectively. The bearing shaft was manufactured using heat treatment of the bearing steel, whereas the bearing housing was processed using a urethane rod. The outer diameter of the bearing housing was 24 mm, and a groove of 1 mm was provided in its center for winding tungsten wire. Fig. 6 shows the bearing, bearing housing, and shaft used in the experiment.

Table 2 The chemical composition of bearing (wt%)

Description	Bronze (Cu-10wt.%Sn)	Cu	Fe
Sintered bronze	7	20	73

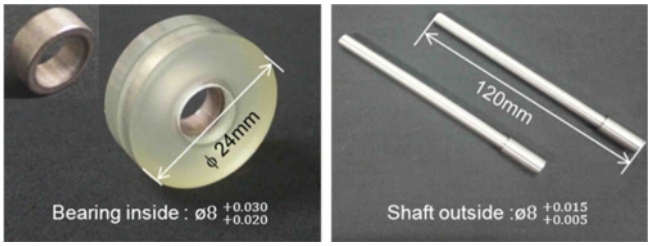

Fig. 6 Bearing, bearing housing, and shaft used in the experiment

First, a basic experiment was conducted to measure the COFs of the bearing. The load used to apply tension to the wire was approximately 5 N. The motor was operated (starting and stopping) six times in iterations of 5 s each. The motor rotation speed was maintained at a constant 3,000 RPM. The data from the second to the sixth iterations were used for COFs conversion, whereas the data from the first iteration were excluded owing to the warming-up period. Data were collected 1,000 units per second. Fig. 7 shows the coefficient of static friction and kinetic friction at a motor speed of 3,000 RPM. The coefficient of static friction was generated at the moment the motor started to rotate. A force (F_L) of 5.47 N exerted on the load cell was measured by adding the initial load of approximately 5 N. The coefficient of kinetic friction was generated when the motor was rotated, and F_L of approximately 5.25 N was measured. The standard deviations of the coefficient of static friction and kinetic friction were measured to be uniform values of 0.03 and 0.02, respectively. The COFs was calculated using Eq. (7).

The friction test was initiated once the values of the motor speed, operation time, count, and weight were input. The test was conducted using loads of 5 N and 15 N transferred through the wire, in order to determine the COFs based on an initial load, thereby measuring the COFs under various load conditions. To confirm reliability, the experiment was conducted five times at motor speeds of 1,000~6,000

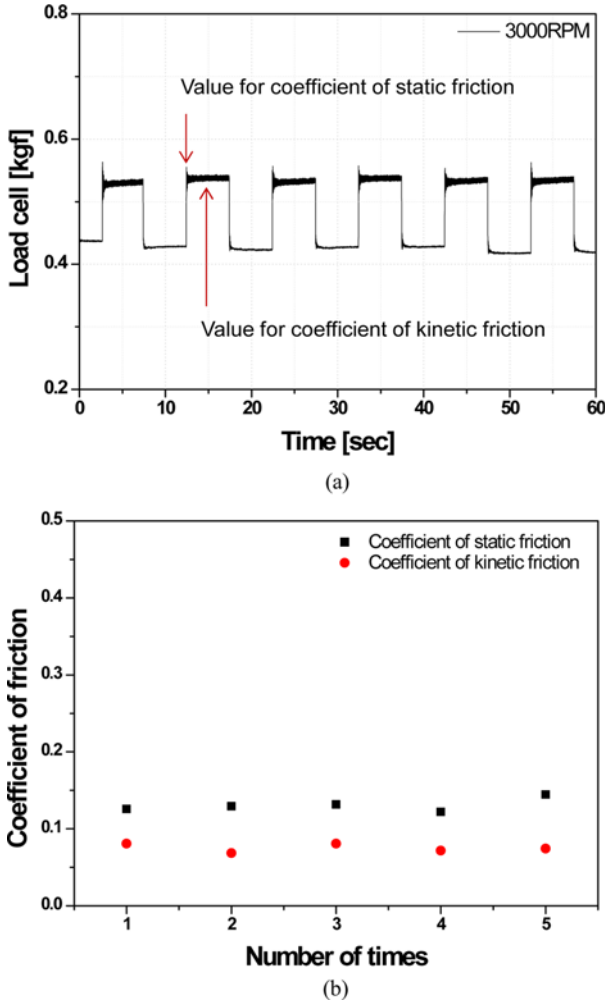

Fig. 7 Basic experiment for COFs at 3000 RPM: (a) load cell data (F_L) for COFs conversion; (b) coefficient of friction

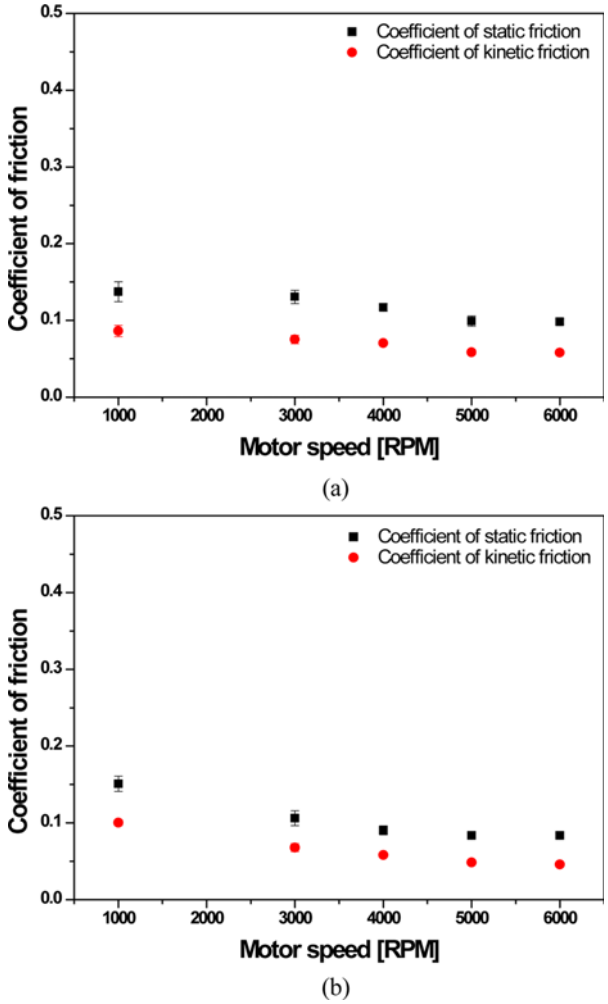

Fig. 8 Experimental results: (a) bearing's coefficient of friction under the initial loading of 5 N; (b) 15 N

RPM in order to measure the average and standard deviation. Fig. 8 shows the graph of the bearing's COFs under the initial loads of 5 N and 15 N. The coefficient of static friction and kinetic friction has decreased as the motor speed increased, at speeds of 1,000, 3,000, 4,000, and 5,000 RPM, i.e., except at the motor speed of 6,000 RPM.

The reason for this was that the main bearing was an oil-impregnated sintered bearing, and hence, a considerable amount of oil was produced and the friction coefficient decreased as the motor speed increased beyond 5,000 RPM. The deviation of the bearing COFs at 2,000 RPM was found to be too large and hence unreliable.

It was excluded from the graph because the bearing friction force could not be accurately calculated owing to vibration of the system. This vibration was due to the resonance with the bearing tester. Furthermore, while applying the initial loads of 5 N and 15 N, the resultant values of the COFs at each RPM showed that the coefficient of static friction under the initial load of 5 N had increased up to 0.027 depending on the RPM. Additionally, the coefficient of kinetic friction had increased up to 0.012, compared to that at the initial load of 15 N. The results of the present study are consistent with the results of the study conducted by Ünlü and Atik, who found that the COFs increased as the load exerted on a bearing under dry conditions was reduced.[12]

Fig. 9 shows the results of the noise measurement performed during

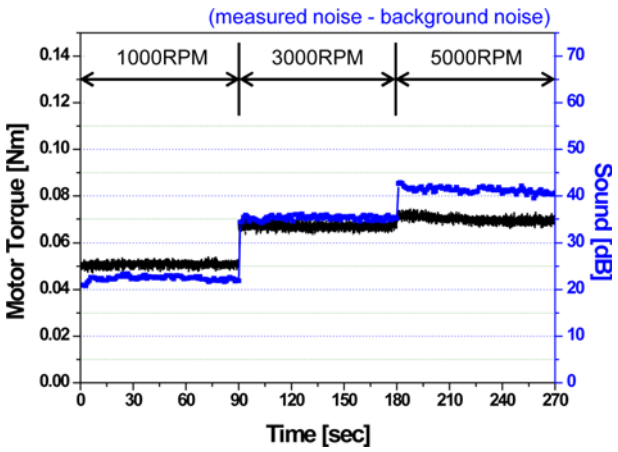

Fig. 9 Noise measurement performed during the operation of the bearing tester

the operation of the bearing tester. The equipment used for the noise measurement was a microphone (GRAS Inc. 40AF) and a signal processor (01dB Inc. Harmonie). The noise was measured at a distance of approximately 10 cm from the bearing tester. The measurement results were calculated by subtracting the background noise from the

measured noise. The measured noises were 22.4, 35.2, and 40.4 dB at speeds of 1,000, 3,000, and 5,000 RPM, respectively. This indicates that the noise increased with increasing motor speed. The resulting noise was equivalent to a conversation-level noise as defined by the daily living noise standard, which ensured that there was no problem in using the tester for industrial equipment.

4. Conclusions

The method for measurement of the bearing COFs proposed in this paper did not use an existing torque sensor, which has a large volume. Instead, it used the wire tension method to measure the COFs of bearings manufactured with various structures, sizes, and materials. Using the wire tension method, the COFs was calculated under different loads and motor speeds. The coefficient of static friction and kinetic friction showed has decreased as the motor speed increased in steps of 1,000, 3,000, 4,000, and 5,000 RPM, except at the motor speed of 6,000 RPM. The reason for this was that the main bearing was an oil-impregnated sintered bearing, so a considerable amount of oil was produced and the COFs decreased as the motor speed increased beyond 5,000 RPM. The COFs values measured under different initial loads showed that the coefficient of static friction and kinetic friction increased more under the initial load of 5 N than under the initial load of 15 N. Furthermore, the result of the noise measurement showed that noise increased as motor speed increased. This result ensured that on the basis of the daily living noise standard, there were no problems in using the tester for industrial equipment.

ACKNOWLEDGEMENT

This work was supported by the Human Resources Development program (No. 20134030200240) of the Korea Institute of Energy Technology Evaluation and Planning (KETEP) grant funded by the Korea government Ministry of Trade, Industry and Energy.

REFERENCES

1. Holmberg, K., Andersson, P., and Erdemir, A., "Global Energy Consumption due to Friction in Passenger Cars," Tribology International, Vol. 47, pp. 221-234, 2012.
2. Yoo, S. Y., Kim, W. Y., Kim, S. J., Lee, W. R., Bae, Y. C., and Noh, M., "Optimal Design of Non-Contact Thrust Bearing using Permanent Magnet Rings," Int. J. Precis. Eng. Manuf., Vol. 12, No. 6, pp. 1009-1014, 2011.
3. Chen, X. D., Zhu, J. C., and Chen, H., "Dynamic Characteristics of Ultra-Precision Aerostatic Bearings," Advances in Manufacturing, Vol. 1, No. 1, pp. 82-86, 2013.
4. Waghole, V. and Tiwari, R., "Optimization of Needle Roller Bearing Design using Novel Hybrid Methods," Mechanism and Machine Theory, Vol. 72, pp. 71-85, 2014.
5. Lingwall, B. A., Sexton, T. N., and Cooley, C. H., "Polycrystalline Diamond Bearing Testing for Marine Hydrokinetic Application," Wear, Vol. 302, No. 1–2, pp. 1514-1519, 2013.
6. Dai, X., Zhang, K., and Tang, C., "Friction and Wear of Pivot Jewel Bearing in Oil-Bath Lubrication for High Rotational Speed Application," Wear, Vol. 302, No. 1–2, pp. 1506-1513, 2013.
7. Durak, E., Kurbanoğlu, C., Bıyıklıoğlu, A., and Kaleli, H., "Measurement of Friction Force and Effects of Oil Fortifier in Engine Journal Bearings under Dynamic Loading Conditions," Tribology International, Vol. 36, No. 8, pp. 599-607, 2003.
8. Yao, Z., Zhang, Q., Tao, Y., and Zhang, X., "A New Approach to Measure the Friction Coefficient of Micro Journal Bearings," Tribology International, Vol. 33, No. 7, pp. 485-489, 2000.
9. Budinski, K. G., "An Inclined Plane Test for the Breakaway Coefficient of Rolling Friction of Rolling Element Bearings," Wear, Vol. 259, No. 7–12, pp. 1443-1447, 2005.
10. Fujii, Y., Maru, K., Jin, T., Yupapin, P. P., and Mitatha, S., "A Method for Evaluating Dynamical Friction in Linear Ball Bearings," Sensors, Vol. 10, No. 11, pp. 10069-10080, 2010.
11. Tevruz, T., "Tribological Behaviours of Bronze-Filled Polytetrafluoroethylene Dry Journal Bearings," Wear, Vol. 230, No. 1, pp. 61-69, 1999.
12. Ünlü, B. S. and Atik, E., "Determination of Friction Coefficient in Journal Bearings," Materials & Design, Vol. 28, No. 3, pp. 973-977, 2007.
13. Bouyer, J. and Fillon, M., "Experimental Measurement of the Friction Torque on Hydrodynamic Plain Journal Bearings during Start-Up," Tribology International, Vol. 44, No. 7–8, pp. 772-781, 2011.
14. Rezaei, A., Ost, W., Paepegem, W., Degrieck, J., and Baets, P., "Experimental Study and Numerical Simulation of the Large-Scale Testing of Polymeric Composite Journal Bearings: Two-Dimensional Modeling and Validation," Tribology Letters, Vol. 37, No. 2, pp. 261-272, 2010.
15. Lee, C. G., Hwang, Y. J., Choi, Y. M., Lee, J. K., Choi, C., and Oh, J. M., "A Study on the Tribological Characteristics of Graphite Nano Lubricants," Int. J. Precis. Eng. Manuf., Vol. 10, No. 1, pp. 85-90, 2009.
16. Yousif, B. F., "Design of Newly Fabricated Tribological Machine for Wear and Frictional Experiments under Dry/Wet Condition," Materials & Design, Vol. 48, pp. 2-13, 2013.
17. Nair, R. P., Griffin, D., and Randall, N. X., "The use of the Pin-on-Disk Tribology Test Method to Study Three Unique Industrial Applications," Wear, Vol. 267, No. 5–8, pp. 823-827, 2009.
18. Wang, L., Zhou, J., Duszczyk, J., and Katgerman, L., "Identification of a Friction Model for the Bearing Channel of Hot Aluminium Extrusion Dies by using Ball-on-Disc Tests," Tribology International, Vol. 50, pp. 66-75, 2012.

19. Camci, F., Medjaher, K., Zerhouni, N., and Nectoux, P., "Feature Evaluation for Effective Bearing Prognostics," Quality and Reliability Engineering International, Vol. 29, No. 4, pp. 477-486, 2013.

20. Allmaier, H., Priestner, C., Six, C., Priebsch, H. H., Forstner, C., and Novotny-Farkas, F., "Predicting Friction Reliably and Accurately in Journal Bearings-A Systematic Validation of Simulation Results with Experimental Measurements," Tribology International, Vol. 44, No. 10, pp. 1151-1160, 2011.